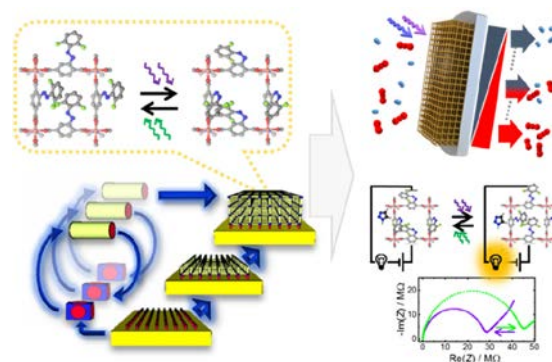


# Photoswitchable Metal–Organic Framework Thin Films: From Spectroscopy to Remote-Controllable Membrane Separation and Switchable Conduction

Yunzhe Jiang and Lars Heinke\*

**ABSTRACT:** The preparation of functional materials from photo switchable molecules where the molecular changes multiply to macroscopic effects presents a great challenge in material science. An attractive approach is the incorporation of the photoswitches in nanoporous, crystalline metal–organic frameworks, MOFs, often showing remote controllable chemical and physical properties. Because of the short light penetration depth, thin MOF films are particularly interesting, allowing the entire illumination of the material. In the present progress report, we review and discuss the status of photoswitchable MOF films. These films may serve as model systems for quantifying the isomer switching yield by infrared and UV–vis spectroscopy as well as for uptake experiments exploring the switching effects on the host–guest interaction, especially on guest adsorption and diffusion. In addition, the straightforward device integration facilitates various experiments. In this way, unique features were demonstrated, such as photoswitchable membrane separation with continuously tunable selectivity, light switchable proton conductivity of the guests in the pores, and remote controllable electronic conduction.



## INTRODUCTION

Remote controllable, also referred to as smart, materials can change their structures and properties upon exposure to external stimuli such as heat, pH, redox potential changes, and light irradiation.<sup>1–7</sup> Switching by light is particularly desirable, allowing clean, typically nondestructive, fast remote control that is easy to regulate and dose. A highly attractive approach for realizing photoresponsive materials is based on the incorporation of photoswitchable molecules, which isomerize to a different (meta)stable form upon irradiation with light of a certain wavelength and isomerize back to their thermodynamically stable form upon irradiation with another wavelength or by thermal relaxation.<sup>8–11</sup> Representative and intensively investigated photoswitchable molecules are azobenzene (AB), spiropyran (SP), and diarylethene (DAE) (Figure 1a).<sup>12</sup> The changes in their structures substantially affect their properties, including the bond angle, dipole moment, and conjugation, enabling a large range of applications. To date, these molecules have been incorporated into different materials such as polymers<sup>13</sup> and liquid crystals<sup>14</sup> and were explored for various applications. In recent years, their incorporation in modular framework materials, such as metal–organic frameworks (MOFs) and covalent organic frameworks (COFs), has been explored.<sup>15–17</sup>

MOFs, also referred to as porous coordination polymers, are a class of crystalline, porous solids, made from metal containing

nodes connected by organic linkers.<sup>18,19</sup> Since most organic molecules can be functionalized with additional groups such as –COOH and pyridine so that these molecules may serve as potential MOF linkers, these materials are designable to a large extent. In this way, MOFs with unique properties can be designed to possess very high porosity,<sup>20</sup> low density,<sup>21</sup> tunable pore sizes,<sup>22</sup> and high thermal and chemical stability.<sup>23</sup> This allows various applications in adsorption, separation, sensing, and drug loading/release.<sup>18</sup>

Commonly, MOFs are prepared in the form of powders by solvothermal synthesis. For many applications, such as membrane separations, MOF materials in the form of thin films are required. Traditional solvothermal methods including *in situ* growth and seeding methods often allow the synthesis of dense and defect free membranes.<sup>24–29</sup> In 2007, a novel strategy based on layer by layer (lbl) synthesis of MOF thin films directly on modified substrate surfaces was introduced, resulting in surface mounted MOFs, SURMOFs (Figure 1b).<sup>30–33</sup> There, the substrate is sequentially exposed to a solution of the metal

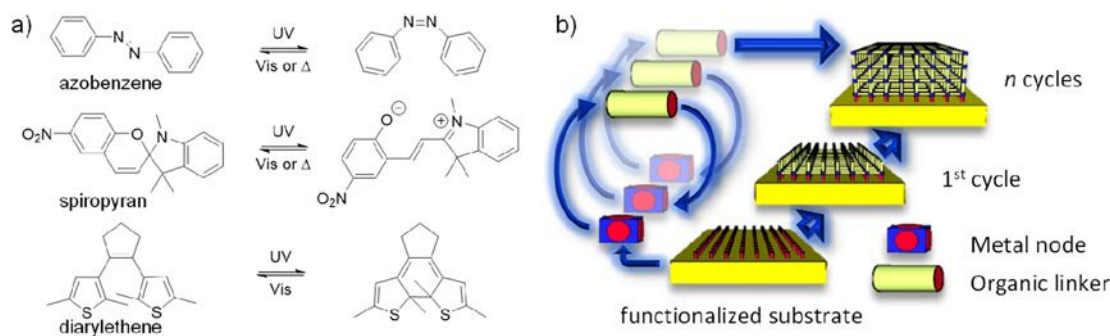


**Figure 1.** (a) Structures of azobenzene (AB), spiropyran (SP), and diarylethene (DAE) and their light induced isomerization. The thermodynamically more stable form is shown on the left hand side. (b) Schematic illustration of the layer by layer synthesis of SURMOFs on a modified substrate. Panel b was adapted with permission from ref 44, copyright Wiley VCH (2019).

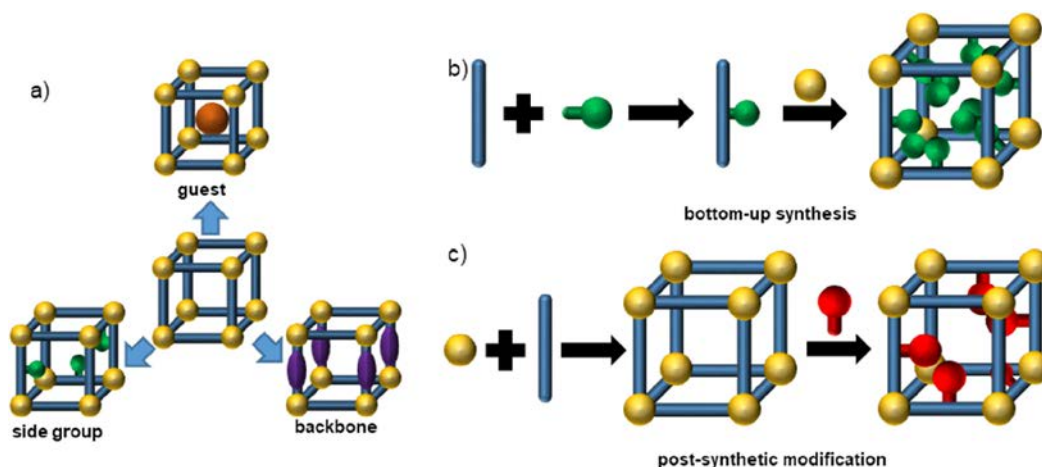


**Figure 2.** (a) Methods for incorporating photoresponsive molecules in MOFs: brown, guests; green, side groups; and purple, backbone. The yellow spheres symbolize the metal nodes, and the blue sticks, the linker molecules. Schemes of (b) bottom up synthesis and (c) postsynthetic modification, both resulting in MOFs with functional side groups.

nodes followed by a solution of the linker molecules, and after each exposure, the sample is washed to remove unreacted MOF components. SURMOF growth can also be observed *in situ* by a gravimetric technique such as quartz crystal microbalance (QCM)<sup>34</sup> or by a microscopy technique such as atomic force microscopy.<sup>35,36</sup> In comparison to conventional MOF membranes or films, SURMOFs have a controllable thickness,<sup>37,38</sup> a higher and controllable crystalline orientation,<sup>39,40</sup> and a lower defect density.<sup>38,41–43</sup> These properties not only cause SURMOFs to be perfectly suited for various applications but also allow them to be used as an ideal model system for the investigation of adsorption, permeation, and conduction processes.<sup>44</sup>

The controlled, typically very small thickness of the SURMOFs presents a great advantage for the interaction with light, in particular, for optical and vibrational spectroscopy and for light illumination. For MOF powders, UV–vis or infrared (IR) spectroscopy in transmission mode is hampered by its low transparency, and typically complex techniques are required. For example, UV–vis spectroscopy with MOF powders requires an integrating sphere, which is expensive, and the signal to noise ratio is typically low compared to the results from a transmission method. For IR spectroscopy of MOF powders, the material is typically pressed into pellets using potassium bromide binder, leading to a destruction of the sample. Alternatively, attenuated total reflection (ATR) IR methods can be used, avoiding sample destruction. However, the irradiation (i.e., photoswitching) and

the investigation of the isomerization in exactly the same part of the sample are barely possible. In contrast, for thin SURMOF films, IR and UV–vis spectra can be recorded in transmission mode when prepared on a transparent substrate such as quartz glass or calcium fluoride<sup>42,45,46</sup> and in reflection–absorption mode when prepared on a reflecting substrate such as gold.<sup>47–49</sup> These methods, where special sample preparation is avoided, typically cause no damage to the sample and allow high signal to noise ratios, making SURMOFs ideally suited for spectroscopic investigations.

For photoresponsive materials, the light penetration depth is an important parameter, governing the range where the material is switched. The absorbance of dyes and photochromic molecules is typically strong, so MOFs with a high density of such molecules have short light penetration depths, typically in the range of a micrometer. As a result, the illumination of powders or pellets of MOFs containing photoswitches causes only a photoresponse in the outer layer of the material. In contrast, SURMOF films with thicknesses in the range of 100 nm are fully illuminated, causing the entire MOF material to undergo photoisomerization.

For conductive MOFs, the physical form of MOFs such as pressed pellets, thin films, and single crystals has a great influence on the measured value of the electrical conductivity.<sup>50</sup> Most of the measurements are based on pellets because of their straightforward preparation. However, the sizes of crystals, the boundaries between the MOF crystals, and the orientations

**Table 1. Summary of Photoswitchable MOF Films**

MOF film	switchable moiety	position	photoswitching applications	ref
$\text{Cu}_2(\text{BDC})_2(\text{AzoBiPyB})$	AB	side group	alkane and alcohol adsorption	56
$\text{Cu}_2(\text{DCam})_2(\text{AzoBiPyB})$	AB	side group	enantioselective adsorption	57
AB@HKUST-1 and tfAB@HKUST-1	AB and fluorinated AB	guest	butanediol adsorption	58
series of AB-based pillared-layer SURMOFs	AB	side group	butanol adsorption	59
$\text{Cu}_2(\text{AZoBPDC})_2(\text{BiPy})$	AB	side group	butanediol diffusion and release	49
$\text{Cu}_2(\text{AZoBPDC})_2(\text{AzoBiPyB})$	AB	side group	$\text{H}_2/\text{CO}_2$ membrane separation	60
AB@UiO-67	AB	guest	$\text{H}_2/\text{CO}_2$ membrane separation	61
$\text{Cu}_2(\text{F}_2\text{AzoBDC})_2(\text{dabco})$	fluorinated AB	side group	$\text{H}_2/\text{C}_3\text{H}_6$ membrane separation	62
$\text{Cu}_2(\text{F}_2\text{AzoBDC})_2(\text{dabco})$	fluorinated AB	side group	proton conduction	63
$\text{Cu}_2(\text{SP-BPDC})_2(\text{dabco})$	SP	side group	proton conduction	64
SSP@ZIF-8	sulfonated SP	guest	proton conduction	65
SSP@ZIF-8	sulfonated SP	guest	lithium ion conduction	66
SP@UiO-67	SP	guest	electron conduction	67
$\text{Cu}_2(\text{BDC})_2(\text{AzoBiPyB})$ and $\text{Cu}_2(\text{DMTPDC})_2(\text{AzoBiPyB})$	AB	side group	exploring isomerization and energy barrier	68
$\text{Cu}_2(\text{AZoBPDC})_2(\text{BiPy})$ and $\text{Cu}_2(\text{NDC})_2(\text{AzoBiPy})$	AB	side group	exploring isomerization and steric hindrance	69
SP-JUC-120	SP	guest	optical device	70
$\text{Cu}_2(\text{F}_2\text{AzoBDC})_2(\text{dabco})$	fluorinated AB	side group	refractive index and Bragg mirror	71

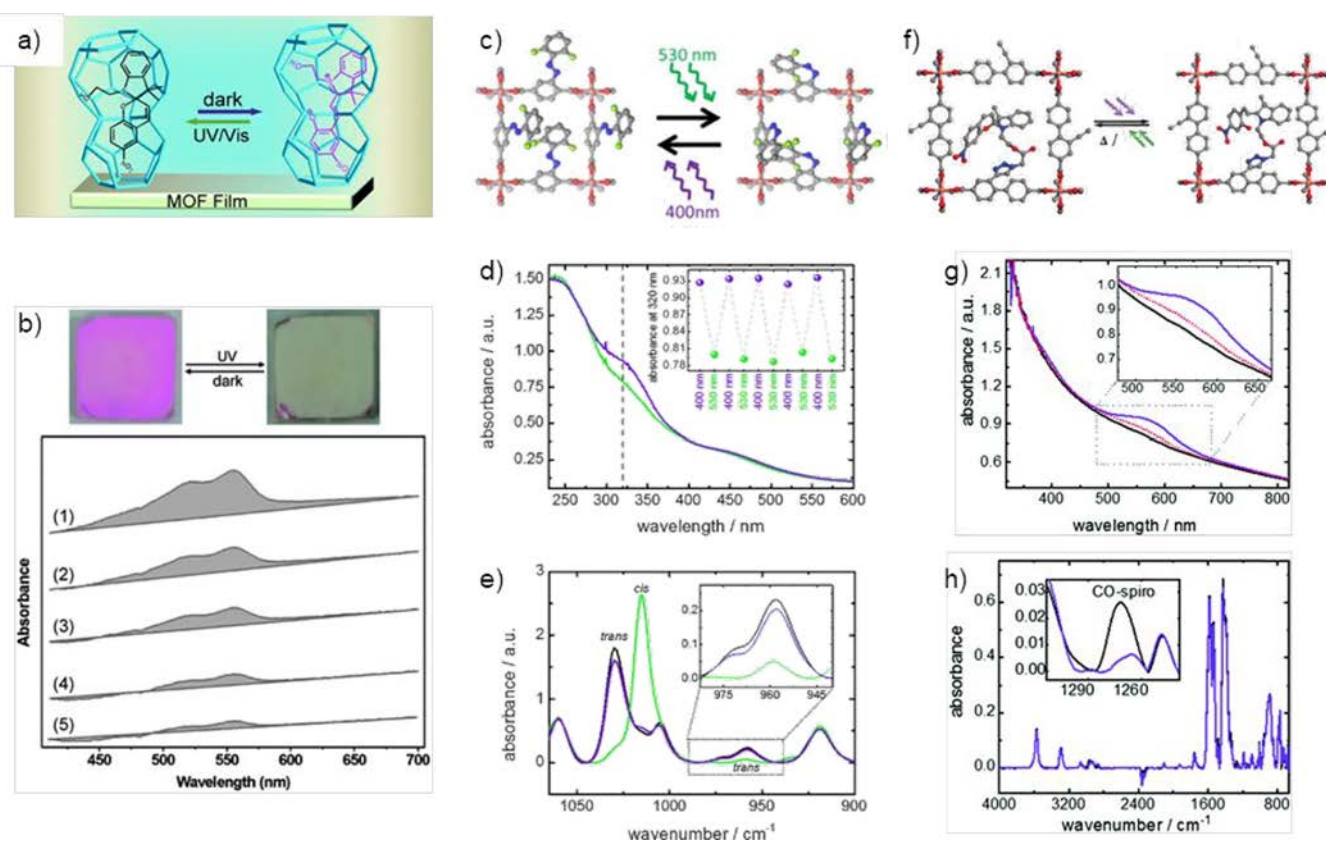


**Figure 3.** (a) Scheme of SP loaded JUC 120. (b) Photograph and UV–vis spectra of SP JUC 120 film upon UV irradiation. SURMOF structures (c) with fluorinated AB side groups made by bottom up synthesis and (f) with SP side groups incorporated into PSM and their photoisomerizations. (d and e) UV–vis and IRRAS spectra of (c). (g and h) UV–vis and IR spectra of (f). Panels (a) and (b), reproduced with permission from ref 70, copyright The Royal Society of Chemistry (2012). Panels (c–e), reproduced with permission from ref 62, copyright Wiley VCH (2017). Panels f–h), reproduced with permission from ref 64, copyright The Royal Society of Chemistry (2020).

affect the measurements.<sup>51</sup> Avoiding these shortcomings, thin films may represent a valuable alternative, also allowing their incorporation in practical devices.<sup>52</sup>

To date, a variety of photoswitchable smart thin films have been reported. In the present progress report, we review the state of the art of photoswitchable MOF films and membranes with a special emphasis on SURMOFs. Different investigations and applications are discussed. We discuss the assets and drawbacks

of photoswitchable SURMOFs and give a subjective prospect of future trends.

### INCORPORATION OF PHOTOCHROMIC MOLECULES AND SPECTROSCOPY

Principally, there are three different methods for incorporating photoswitchable molecules in MOFs: loading them as guests in

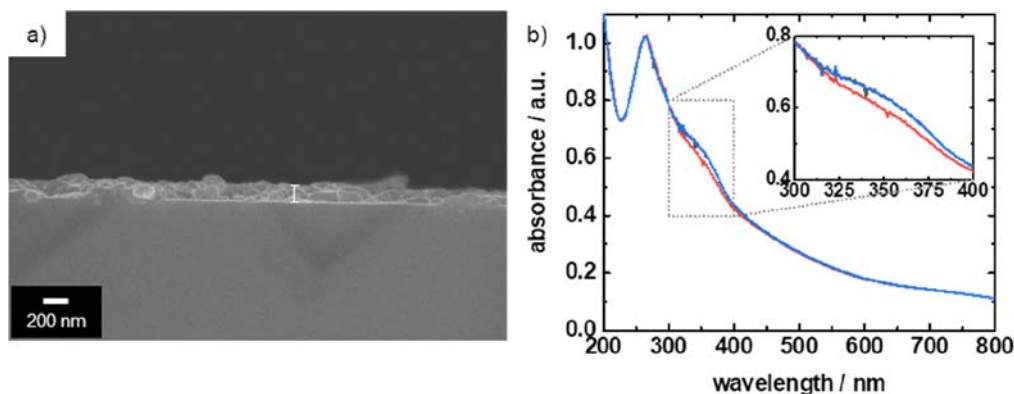


**Figure 4.** (a) SEM picture of  $\text{Cu}_2(\text{BDC})_2(\text{AzoBiPyB})$  SURMOF on quartz glass. The film thickness is approximately 150 nm. The sample was broken, and the broken surface is imaged. (b) UV–vis spectra of the same SURMOF sample measured in transmission mode. The sample is in the pristine state (*trans*, black), irradiated with UV light of 365 nm (red) and with 455 nm light (blue). The intensity change of the  $\pi\text{--}\pi^*$  band is shown in the inset. The black and blue spectra are virtually identical.

the pores, grafting them as side groups to the scaffold, and incorporating them in the MOF backbones (Figure 2a). Although MOF powders with photoswitchable components such as DAE in the backbone have been presented,<sup>53–55</sup> to the best of our knowledge the photoswitching of the backbone has not yet been shown for a MOF film. Here, only the first two methods are discussed: as side groups and as guests in MOF films where the responsive molecules are AB and SP (Table 1).

**Photoswitchable Molecules as Guests.** Because most photoswitchable molecules are commercially available, a straightforward way to realize photoswitchable MOFs is to load the functional molecules in the pores, referred to as photoswitch@MOF approach. This method avoids the (potentially complex) organic synthesis of the photoswitchable linkers. In some (SUR)MOF structures such as HKUST 1 (abbreviation for Hong Kong University of Science and Technology), made of 1,3,5 benzenetricarboxylic acid and copper dimers, there is no opportunity presented for adding further functional groups at the linker, but their pore space can be used as a host. When photoswitchable molecules serve as guests, the photoswitching properties or the interactions between them and the MOF (host–guest) are not interfered with by covalent bonds. The major factor is the size of the guest molecule, which should be smaller than the MOF pore size. Alternatively, the photoswitch can be embedded during the synthesis,<sup>65</sup> or an *in situ* embedment<sup>72</sup> can be used. Such a synthesis is sometimes also referred to as “bottle around the ship” synthesis.

To date, ABs and SPs have been successfully loaded into MOF thin films. For example, AB has been loaded into HKUST 1 SURMOF for remote controllable guest uptake by straightforward immersion of the SURMOF sample in AB solution. Both UV–vis and IR spectra prove a high AB loading in the SURMOF pores, and the optical properties of AB in the SURMOF match well with AB in solution.<sup>58</sup> SP is another common molecule where the photoisomerization between the closed SP form and the open merocyanine (MC) form goes along with large structural changes, making it unsuitable for incorporation into the MOF backbone. MOFs with a structure termed JUC 120 (abbreviation for Jilin University China), made of 1,3,5 benzenetricarboxylic acid and  $\text{In}(\text{NO}_3)_3$ , were loaded with SP during the synthesis (Figure 3a,b).<sup>70</sup> The MOF film was prepared by spin coating the SP@MOF suspension onto the quartz substrates. In another example, UiO 67 was used as host

to embed SP, where 7.5 SP molecules were loaded in each MOF unit cell of  $(2.6 \text{ nm})^3$ .<sup>67</sup>

The molecular properties, in particular, the photophysical features, of the photoswitches can be influenced by their molecular environments. Thus, depending on the MOF pore environment and functionality, the embedding in the pores may change the properties of the switches. So, the MOFs can be described as “solid solvents”.<sup>73–75</sup> The loading of guest molecules can also significantly decrease the pore volume of MOFs. A high loading of guest molecules may result in dense packing, hindering possible photoswitching.<sup>61</sup>

**Photoswitchable Side Groups.** For molecules with large conformation changes, such as AB and SP, their incorporation into the backbone of the MOF scaffold sterically hinders the photoisomerization.<sup>76</sup> On the other hand, the incorporation of such switches as side groups pendant to the MOF structure typically offers enough space for the molecular isomerization.<sup>77</sup> The photoswitchable side groups can be attached to the MOF linker prior to MOF synthesis, which is referred to as “bottom up synthesis” (Figure 2b), or they can be incorporated as side groups after MOF synthesis, referred to as postsynthetic modification (PSM) grafting (Figure 2c). Using AzoBiPyB linker molecules, which are (*E*) 2 (phenyldiazenyl) 1,4 bis(4 pyridyl)benzene, having AB as a side group allows the direct bottom up synthesis of photoswitchable pillared layer SURMOF. UV–vis spectroscopy data indicate that the AB switching behavior in the SURMOF is essentially identical to the behavior in ethanolic solution.<sup>57,68</sup> Fluorinated azobenzene<sup>78</sup> was used for synthesizing similar pillared layer SURMOF (Figure 3c–e), avoiding the switching by harmful UV light.<sup>62</sup>

In some cases (e.g. when the bottom up synthesis fails or to avoid the complex organic synthesis of the photoswitches), PSM<sup>79</sup> methods are beneficial, which means first synthesizing the MOF with active functional groups and then grafting the photoswitching side groups, typically by click chemistry (Figure 2c). For example, azide functionalized SP was grafted via click chemistry<sup>80</sup> in alkynyl containing SURMOFs after its synthesis (Figure 3f–h).<sup>64</sup> The SURMOF remained stable after PSM, and an average of 0.83 spiroopyran molecule was anchored in each MOF pore. In general, the density of side groups grafted by PSM is smaller than that in the bottom up synthesis, which in some cases may reduce the steric effects for side groups that are too large.

The covalent bonding of the photoswitch at the MOF scaffold results in stable photoswitchable materials. In different experiments using SURMOFs with plain AB and fluorinated AB photoswitches,<sup>56,57,62,63,68</sup> no significant photobleaching effect was observed for many, often more than 50, irradiation cycles. This indicates the stability of the material. On the other hand, for the photoswitch@MOF approach, the guest molecules may desorb (slowly) from the pores. For AB@HKUST 1, it was found that the desorption is very slow and a depletion time constant of at least several months was estimated.<sup>58</sup>

## SPECTROSCOPIC INVESTIGATIONS AND QUANTIFICATIONS OF THE SWITCHING YIELD

The color changes, necessarily correlated with changes in UV–vis absorption spectra, are fundamental features of photochromic or photoswitchable molecules. For plain AB, an intense absorption band at approximately 320–350 nm, caused by a  $\pi$ – $\pi^*$  transition, is observed for the *trans* and *cis* isomers; however, the intensity of the *trans* isomer is significantly stronger.<sup>81</sup> On the other hand, the  $n$ – $\pi^*$  transition at roughly 430 nm for the *cis* isomer is significantly larger than of the *trans* isomer. For SP, the adsorption band at 272–296 nm is attributed to the  $\pi$ – $\pi^*$  transition in the indoline part and 323–351 nm in the chromene part of the SP molecule. After UV induced isomerization to the MC form, a new band at around 550–600 nm occurs due to the extended  $\pi$  conjugated system between the indoline and the chromene moieties.<sup>82</sup> The wavelength of this rather wide band may depend on the molecular environment.<sup>74</sup> By comparing the absorbance changes at specific wavelengths, the isomerization in photo switchable materials can be verified.

UV–vis spectroscopy of SURMOF is typically performed in transmission mode, similar to the measurement of photo switchable molecules in solution, allowing a direct comparison between the photoswitching of the functional moieties in solution and in the MOF.<sup>9</sup> For example, the UV–vis transmission spectra of a SURMOF of  $\text{Cu}_2(\text{BDC})_2(\text{AzoBiPyB})$  structure are shown in Figure 4. The scanning electron microscopy (SEM) images of the sample show that the SURMOF thickness  $l$  is approximately 150 nm.

The light penetration depth  $\delta_p$ , which is defined as the depth at which the light intensity in the material decreases to  $1/e$  ( $\sim 37\%$ ) of its original value, can be calculated with  $\delta_p = l/(A \ln 10)$ .  $A$  refers to the absorbance, as shown in the UV–vis spectra. For the MOF film in Figure 4, the penetration depth at 365 nm, which is the typical wavelength used for *trans* to *cis* AB photoswitching, is about 110 nm. As a result, the absorbance of a 1  $\mu\text{m}$  thick film is approximately 4, meaning only a light fraction of 0.0001 can penetrate the film. This means that for an MOF powder or pellet only the volume close to the outer surface of roughly 1  $\mu\text{m}$  thickness is irradiated and photoswitched. Since the SURMOF thickness is typically in the range of a few tens to a few hundred nanometers, light penetration of the entire sample is realized.

UV–vis spectra have been widely used in monitoring the photoswitching of AB and SP in SURMOFs. The UV–vis spectra of a fluorinated AB SURMOF are shown in Figure 3d. The spectra exhibit photoswitching behavior similar to that of the linker in solution, that is, switching from *trans* to *cis* under 530 nm irradiation and switching back under 400 nm irradiation.<sup>62</sup>

UV–vis spectra of SP containing MOF films, either SP embedded in a spin coated JUC 120 film or SP incorporated by

PSM in SURMOFs, are shown in Figure 3b and g. In the SURMOF sample, the increase of the MC band at approximately 550 nm upon UV irradiation is clearly visible, verifying the SP to MC isomerization. For the SP embedded in JUC 120, the MC form is thermodynamically more stable and an intensity decrease in the MC band upon light irradiation, indicating MC to SP isomerization, is observed.

The yield of the photoisomerization is typically below 100%, and the quantification of the isomer composition of the sample upon irradiation, referred to as the photostationary state (PSS), is important.<sup>83</sup> Because of typically overlapping UV–vis absorption bands of both isomers and problems of determining the baseline in the UV–vis spectra, the composition at the PSS by UV–vis spectroscopy is rarely possible. Methods such as nuclear magnetic resonance (NMR)<sup>84</sup> and chromatography<sup>85</sup> can be used for the isomer quantification. A straightforward nondestructive method is based on IR spectroscopy, enabled by the transparency of the MOF material over a wide IR range and the nonoverlapping IR bands of the isomers. It is noteworthy that other photoswitchable materials such as polymers and liquid crystals are typically IR nontransparent, hindering IR spectroscopy. The IR spectra of SURMOFs can be measured by IR reflection absorption spectroscopy (IRRAS) without destroying the sample, enabling the quantification of the switching yield in the PSS. For example, in the IR spectrum of fluorinated AB SURMOFs (Figure 3e), the vibrational bands at  $960\text{ cm}^{-1}$  can be assigned to the *trans* state. Initially, the sample is thermally relaxed (i.e., 100% *trans*), and the area under the  $960\text{ cm}^{-1}$  band decreases by 87% after irradiation with green light. Upon subsequent violet light irradiation, 86% is restored. This indicates that the *trans*:*cis* PSS values are 13%:87% and 86%:14% upon green and violet light irradiation, respectively, in very good agreement with the switching yield of the linker molecules in solution.<sup>62</sup>

The switching yield of SP in SURMOFs can be quantified in a similar way (Figure 3h). Upon UV light irradiation, 80% of the SP molecules isomerize to the MC state.

Apart from quantifying the switching yield, IR spectroscopy can be used to explore the transient behavior of the photoswitches. In this way, the thermal relaxation rates and activation energies can be quantified. In a large pore MOF with isolated AB side groups, an activation energy of  $1.09 \pm 0.09\text{ eV}$  was determined for the thermally activated *cis* to *trans* relaxation.<sup>68</sup> It was suggested that this MOF may act as a model system for isolated AB moieties, avoiding solvent effects. While the former study was performed in vacuum, using SURMOFs in combination with surface plasmon resonance (SPR) also allows us to explore the AB relaxation in various gas atmospheres or solvents.<sup>86</sup>

## PHOTOSWITCHABLE HOST–GUEST INTERACTION

Because of their high porosity, specific surface area, and designable pore structure, MOFs are very promising candidates in the field of molecular storage and separation.<sup>87,88</sup> By incorporation of photoswitchable molecules, the sizes of the pores and pore windows can be modulated, allowing remote control of the uptake and of the mass transfer. AB is most commonly used in these applications owing to its apparent simplicity and its molecular properties, including shape, polarity, and dipole moment changes upon irradiation.<sup>77</sup> These changes may have versatile influences on the host–guest interactions: in addition to changing the pore and window size,<sup>61,62</sup> it may

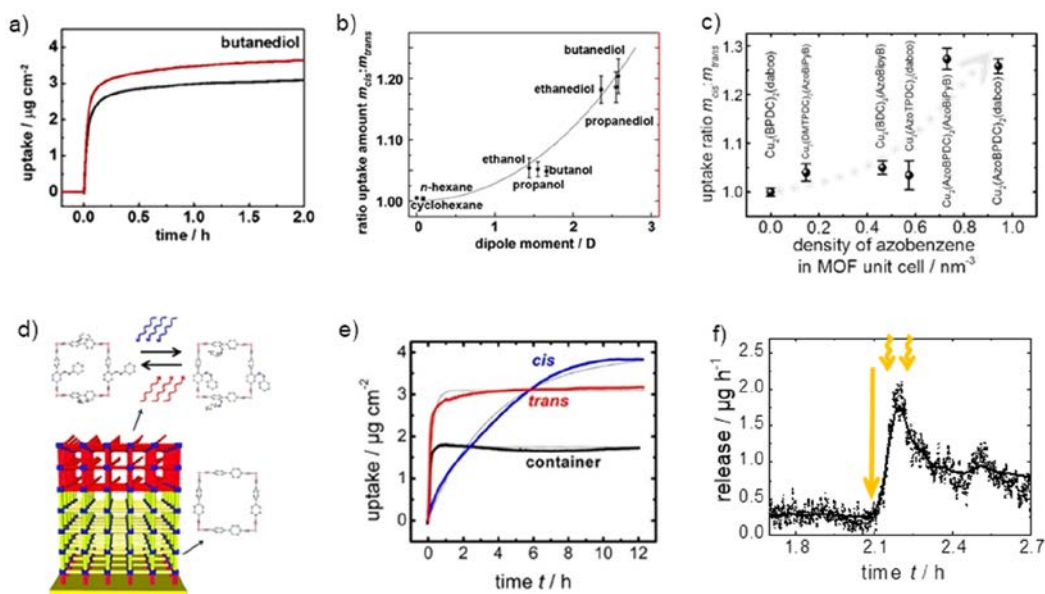


**Figure 5.** (a) Butanediol uptake by photoswitchable  $\text{Cu}_2(\text{BDC})_2(\text{AzoBiPyB})$  measured by QCM. The black line is for the *trans* state, and the red line is for the *cis* state. (b) Ratio of *cis/trans* uptake amounts of various molecules in  $\text{Cu}_2(\text{BDC})_2(\text{AzoBiPyB})$  SURMOF plotted as a function of the dipole moments of the guest molecules. (c) Ratio of *cis/trans* uptake amounts of butanol in different AB SURMOFs versus the AB density per volume in the SURMOF. (d) Sketch of a two layered SURMOF with a passive (not switchable) bottom layer and a photoswitchable AB top layer. (e) Butanediol uptake by the two layered SURMOF in the *trans* state (red) and in the *cis* state (blue), compared with the uptake by the blank bottom layer SURMOF (black). (f) Butanediol release from the two layered SURMOF. Initially, the pores are filled with the guests and the top layer is in the *cis* state (closed). Under visible light irradiation, indicated by arrows, the top layer switches to the *trans* state (i.e., it opens). The molecules are released, and the mass change is recorded by QCM. Panels (a) and (b), adapted with permission from ref 56, copyright Wiley VCH (2015). Panel (c), adapted with permission from ref 59, copyright American Chemical Society (2018). Panels (d–f), adapted with permission from 49, copyright American Chemical Society (2014).

change the attractive interaction toward the guests<sup>56</sup> and block the access to attractive adsorption sites.<sup>89</sup>

#### Photoswitching the Uptake, Release, and Diffusion.

Investigations on the uptake and release of molecules in porous materials are closely related to practical applications such as gas storage and separation.<sup>90</sup> SURMOFs are excellent research templates for their controlled thickness, controllable defect density, and homogeneous morphology.<sup>44</sup> The adsorption of important gas molecules such as  $\text{CO}_2$ <sup>91</sup> or volatile organic compounds (VOCs) such as hexane and toluene<sup>92</sup> in SURMOFs has been investigated. The amount of molecules adsorbed in MOF films is usually quantified with a quartz crystal microbalance (QCM) (Figure 5a), which can measure small mass changes with sufficient time resolution.<sup>34,93,94</sup> Controllable uptake and release experiments go one step beyond, and the MOF thin film is switched during the experiment. For instance, the uptakes of similar organic vapors by an AB SURMOF in the *trans* or *cis* state were investigated. The results indicate that the dipole moment of the guest molecules plays the leading role in adsorption switching while the molecular size has no significant impact unless the pore size is too small (Figure 5b).<sup>56</sup>

For a series of AB based pillared layer SURMOFs with different pore sizes and different numbers of AB side groups, the photoswitchable adsorption capacities for butanol were measured by QCM. It was found that the density of AB per pore volume is the most important factor in the *cis/trans* uptake ratio rather than the pore size or the number of AB molecules per pore (Figure 5c).<sup>59</sup>

Taking advantage of recording the UV–vis and circular dichroism (CD) spectra in transmission mode,<sup>95</sup> the impact of photoswitchable molecules in a chiral SURMOF was studied. By combining photoswitchable AzoBiPyB as pillar linkers and chiral

D camphoric acid as layer linkers, a SURMOF which has both photoswitchable and chiral properties was reported.<sup>57</sup> For the adsorption of (*S*) or (*R*) phenylethanol, the SURMOF switches between essentially nonselective and enantioselective by light irradiation. In detail, the uptake of (*S*) phenylethanol is approximately 2.9 times larger than the uptake of (*R*) phenylethanol in the *trans* state of the SURMOF, while there is nearly no enantioselective adsorption in the *cis* state. It is noteworthy that the enantioselectivity is modified without modifying the chirality, as proven by the CD spectra.

Apart from the adsorption quantity, the diffusion properties of guest molecules in the MOF pores are pivotal for applications in molecular separation and catalysis, so the remote control of the transportation attracts substantial interest. An early demonstration is a two layered SURMOF where the (passive) bottom layer possesses no photoresponsive components while the top layer has an identical MOF scaffold that is decorated with AB side groups. Butanediol uptake experiments show that the diffusion in the SURMOF with the AB groups in the *trans* state is roughly 15 times faster than in the *cis* state. Since the channel width of the SURMOF barely changes during the isomerization, the diffusion change was attributed to the dipole moment change of AB. The dominating effect of the polarity change in MOFs with AB side groups was also found for the diffusion of  $\text{CO}_2$  using powders and polarity sensitive dyes.<sup>84</sup>

In the two layered MOF film, butanediol is more strongly adsorbed at *cis* AB than at *trans* AB, slowing down the diffusion. By switching the top layer from slow diffusion (closed) to fast diffusion (open), the remote controlled release of guests from a molecular container was demonstrated (Figure 5d–f).<sup>49</sup> In this general approach, various active substances such as small

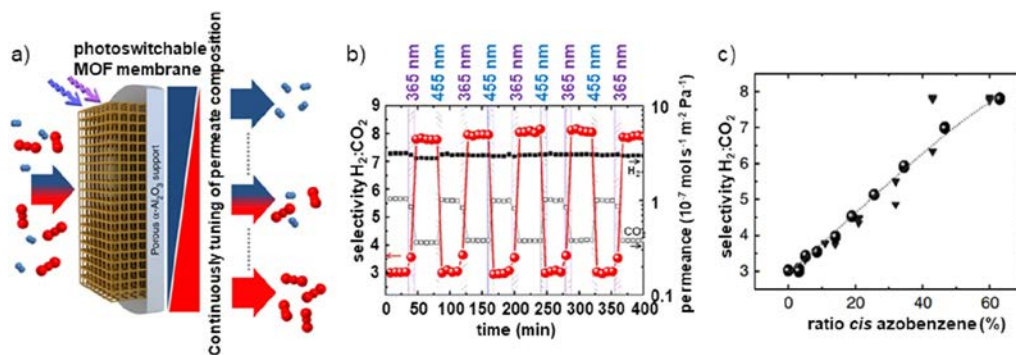


**Figure 6.** (a) Scheme of photoswitchable membrane separation of  $H_2$  and  $CO_2$ . (b) Selectivity and permeance of  $CO_2/H_2$ . The data are measured continuously, and the membrane is irradiated with UV and blue light as labeled. While the  $H_2$  permeation is barely affected by the *trans*–*cis* switching, the  $CO_2$  permeance decreases significantly, leading to reversible switching of the separation factor. (c) Separation factor as a function of the ratio of *cis* AB. Taken with permission from ref 60, copyright Springer, Nature (2016).

pharmaceutical molecules could be embedded in the MOF film and released by irradiation.

**Photoswitchable Membrane Separation.** Separation of liquid or gas mixtures by membranes is very promising for reducing the energy consumption and increasing the efficiency. Generally, the performance of membrane separation is determined by two factors: selectivity (also called the separation factor for membranes) and permeability (representing the flux). MOFs are a strong competitor in the field of membrane separation because of their high porosity, adjustable pore size, and functionalization.<sup>25,96–101</sup> In comparison to conventional MOF membranes made by solvothermal methods, the thickness of SURMOF membranes can be straightforwardly controlled.<sup>102</sup> SURMOFs with AB side groups fabricated on a mesoporous support can be used as photoswitchable membranes, allowing the remote control of the permeability of one (or more) components, thereby changing the separation factor. For the separation of  $H_2/CO_2$ , the separation factor was reversibly switched between 3 in the *trans* state to 8 in the *cis* state (Figure 6). The switching effect is based on dipole moment changes, where the  $CO_2$  permeability is reduced in the *cis* state but the  $H_2$  permeability is barely affected. By adjusting the *cis/trans* ratio, the separation factor can be continuously tuned (Figure 6c).<sup>60</sup> In further experiments, in order to avoid the use of UV light, SURMOFs with fluorinated AB were used. By illumination with green and violet light, the AB can switch between *cis* and *trans*, and the selection factor of the membrane can switch between 9 and 13 for the separation of hydrogen and propene.<sup>62</sup>

A straightforward approach was realized by loading a solvothermally synthesized MOF membrane of UiO 67 structure with AB.<sup>61</sup> Upon adjusting the AB loading, the permeation of the  $H_2/CO_2$  binary gas mixtures was affected by UV and blue light irradiation. The separation factor was photoswitched between 10 and 14.

In a different approach for photoswitchable MOF membranes, AB molecules were incorporated together with 1,2-bis(4-pyridyl)ethylene (4,4' BPE) in the MOF backbone.<sup>103</sup> Under permanent membrane irradiation with either visible or UV light, the separation factor for a  $H_2/CO_2$  gas mixture was modulated between 21.3 and 43.7. The switching mechanism deviates from the above discussed *trans*–*cis* switching, and according to the authors, the AB backbone switching is enabled by distortions and supported by the flexible 4,4' BPE linker. For a better understanding of the switching mechanism and to avoid

the influence of thermal effects, further investigations are required.

Pure MOF membranes suffer from the fact that the preparation of membranes in dimensions required for industrial processes presents a huge challenge and that cracks and pinholes often destroy the performance. A very promising path for industrial applications is the embedding of MOF crystals in polymer matrixes, resulting in mixed matrix membranes (MMMs).<sup>104–106</sup> Recently, photoswitchable MOFs in MMMs were demonstrated.<sup>107,108</sup> For MMMs containing 15 wt % AB based MOF, a decrease of 5–8% after irradiating with UV light was found.<sup>109</sup> Although the presented switching ratio is much smaller than in pure MOF or SURMOF membranes, presumably due to the smaller density of photoswitches, because of its scalability and various options for optimizing the switching effect, this is a very interesting approach.

## CONDUCTION PHOTOSWITCHING

In the past decade, the electronic properties of MOFs and the properties of MOFs as hosts for efficient proton conduction have been extensively explored with respect to various potential applications such as in electronic and optoelectronic devices, sensors, and fuel cells.<sup>110–112</sup>

**Photoswitchable Protonic Conduction.** Proton conductive materials find wide applications in fuel cells<sup>113,114</sup> and sensors.<sup>115</sup> MOFs offer a crystalline porous structure, which can serve as a perfect host for proton conducting molecules. Moreover, the regular pores provide the opportunity to study the proton conduction pathway and mechanism in detail and allow theoretical guidance for the synthesis of new proton conducting materials.<sup>111</sup> To date, both MOF powder pellets<sup>116,117</sup> and thin films<sup>113</sup> with conductivities above  $10^{-2}$  S·cm<sup>-1</sup> under humid conditions have been realized.

By incorporating photoswitchable molecule into the pores, photoswitchable MOFs can be obtained. Remote controllable MOF thin films with fluorinated AB side groups were synthesized on interdigitated electrodes (IDEs), followed by loading with 1,4-butanediol or 1,2,3-triazole. While the host MOF is insulating, the guest molecules are well known proton conductors. For both guest molecules, the proton conductivity reversibly decreases by about 1/3 upon *trans*–*cis* isomerization of the host. DFT calculations and IRRAS measurements indicate that *cis* azobenzene interacts more strongly with –OH or –NH groups of the guest molecules than does the *trans* isomer, leading to smaller mobility and proton conductivity of the guests.<sup>63</sup>

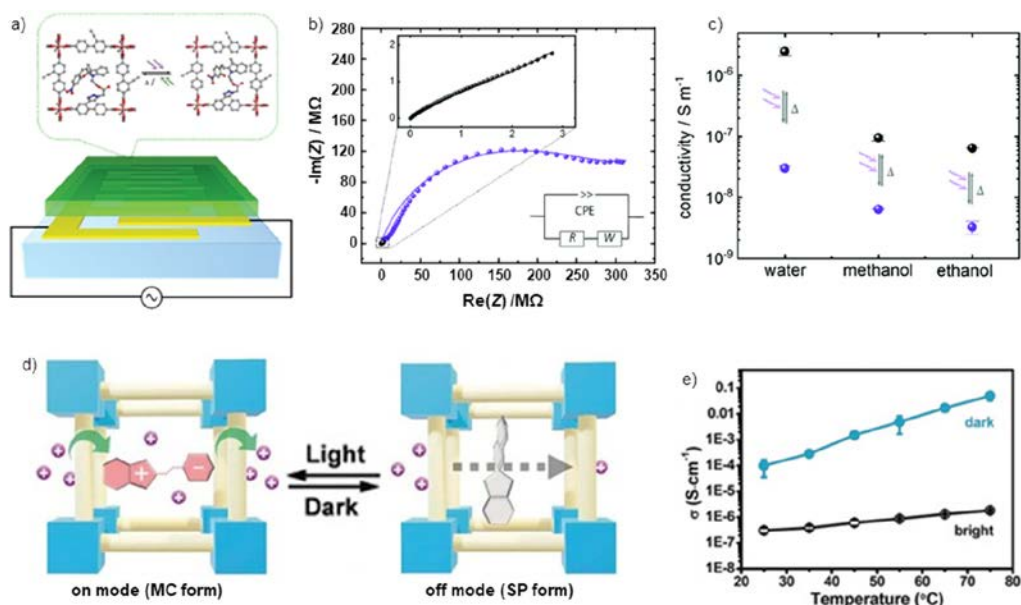


**Figure 7.** (a) Scheme of photoswitchable SP SURMOF on IDE. (b) Nyquist plot of the impedance  $Z$  of the SP SURMOF in a humid environment, with black data points for the pristine SP form and violet data points for the irradiated MC form. (c) Proton conductivities of different guest molecules in the SP SURMOF in the SP form (black) and MC form (violet). (d) Scheme of switchable proton conductivity of SSP@ZIF 8. (e) Conductivity data of SSP@ZIF 8 under light irradiation (bright) and in the dark at different temperatures. Panels (a–c) were reproduced with permission from ref 64, copyright The Royal Society of Chemistry (2020). Panels (d and e), adapted with permission from ref 65, copyright Wiley VCH (2020).

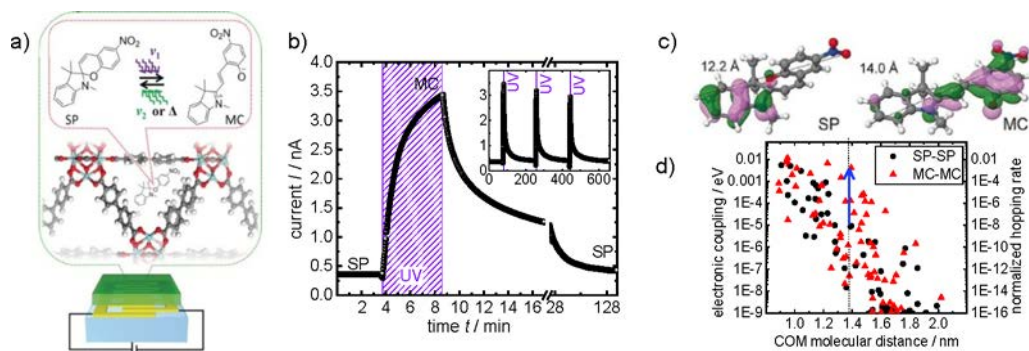


**Figure 8.** (a) Scheme of photoswitchable electronic conduction switching in MOF films with SP guest molecules. (b) DC current versus time at a voltage of 1 V. The current increases by factor 10 after irradiation at 365 nm. Three irradiation cycles are shown in the inset. (c) Structures of SP and MC and visualizations of the highest occupied molecular orbitals (HOMOs). (d) Electronic HOMO coupling between the hopping sites of SP SP and MC MC as a function of their center of mass (COM) distance. Panels (a–d) are adapted with permission from ref 67, copyright Wiley VCH (2019).

To further increase the switching effect, molecules with larger dipole moment changes are required. To this end, SP molecules were grafted in the SURMOF by PSM. Compared to AB with a dipole moment change from 0 to 3 D, the dipole moment change in the SP SURMOF is significantly enhanced, changing from about 5 D (SP form) to about 16 D (MC form). This leads to much stronger hydrogen bonds of the guest molecules with the MC form and also to larger SP MC differences. As a result, a proton conductivity photomodulation by almost 2 orders of magnitude is realized (Figure 7a–c).<sup>64</sup>

By a one pot synthesis, sulfonated spiropyran (SSP) was embedded in ZIF 8 films.<sup>65</sup> There, presumably caused by the polar environment, the open MC form turns out to be thermodynamically stable and the switching to the closed SP form was realized by visible light irradiation. The SSP@ZIF 8 film exhibits high conductivity in the dark, and the conductivity decreased by about 3 orders of magnitude under visible light irradiation (Figure 7d and e). The conductivity change is explained by a hydrogen bond network formed by SSP in the

MC form inside the ZIF 8, allowing efficient proton passage. The hydrogen bond network disappears for the SP form, leading to reduced proton conductivity.<sup>65</sup> The SSP@ZIF 8 membranes were also used to photomodulate the cation transport. The Li<sup>+</sup> conductivity decreases by a factor of 23 upon light induced MC to SP isomerization.<sup>66</sup> The conductivity change is explained by changes in the Li<sup>+</sup> binding sites and in the binding affinity.

**Photoswitchable Electronic Conduction.** Although most MOFs are insulators, some MOFs possess interesting electronic properties with suitable conductivity. For example, MOFs can be designed to be conductive by the incorporation of appropriate coordination bonds between metal nodes and linkers,<sup>118</sup> conjugated  $\pi$ – $\pi$  stacking between organic ligands,<sup>119,120</sup> and the formation of donor–acceptor couples with guest molecules.<sup>121</sup>

Previously, it was shown that the conductivity of SP molecules can be photomodulated by SP MC switching.<sup>122</sup> This is caused by the two separate  $\pi$  electron systems in the indoline and chromene moieties of SP which combine after isomerization to

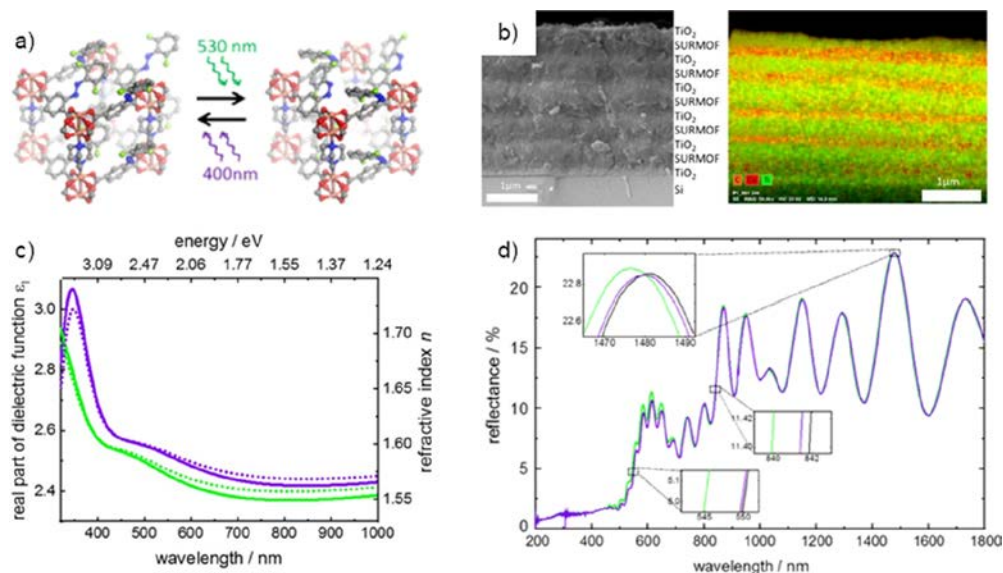


**Figure 9.** (a) Structure of fluorinated AB SURMOF. (b) SEM (left) and EDX (right) of five layers of TiO<sub>2</sub>/SURMOF. In EDX, Cu is shown in red; C, orange; and Ti, green. (c) Real part  $\epsilon_1$  of the dielectric function (dotted lines) of the SURMOF film in the *trans* state (violet line) and in the *cis* state (green line) as determined by ellipsometry. The refractive indexes  $n$ , calculated with  $n^2 = 1/2[\epsilon_1^2 + \epsilon_2^2]^{1/2} + \epsilon_1$ , are shown as solid lines. (d) Reflectance of the sample shown in (b). Black indicates the pristine *trans* sample; green, the *cis* state after green light irradiation; and violet, the *trans* state after subsequent violet light irradiation. Taken with permission from ref 71, copyright American Chemical Society (2019).

MC. Inspired by this phenomenon, nitro substituted SP was used as guest molecules in UiO 67 films synthesized on IDE (Figure 8). DC conduction measurements indicate that after SP to MC isomerization, the conductivity increases 10 fold. Density functional theory (DFT) calculations of the charge transfer mechanism revealed that the increase in conductivity is caused by the larger frontier orbital (i.e., HOMO and LUMO) delocalization in the MC isomer compared to that in SP (Figure 7c). In addition, the molecular extension of the MC isomer is slightly larger than that of the SP isomer. Both effects result in a reduction of the distance between the charge hopping sites, increasing the conductivity. Further calculations predict that an even larger on/off ratio can be realized for MOF structures with optimized distances between SPs.<sup>67</sup>

Although it does not pertain to thin films, a related work on SP MOFs should be discussed where MOF powders and large single crystals with SP were prepared.<sup>53</sup> The powder sample pressed into pellet showed that the conductivity increased by 20% after UV induced SP to MC isomerization while the conductivity of the single crystal increased by only about 5%. The relatively small photoswitching on/off ratio is presumably caused by the small light penetration depth, causing only a small amount of the (thick) sample to undergo photoisomerization. In the same study, DAE was also employed to realize photo switchable conductivity. Photomodulated conductivity based on DAE was previously demonstrated for polymers.<sup>123,124</sup> In ref 53, DAE was incorporated into the MOF backbone, and upon UV induced open to closed photoswitching, the conductivity of the MOF pellets increased by a factor of 2.6. The conductivity change was attributed to the changes in the  $\pi$  conjugation length upon the DAE photocyclization reaction.<sup>53</sup> The realization of such material as a thin film seems very promising.

## REFRACTIVE INDEX SWITCHING

Photonic crystals are regular periodic structures made of materials with different refractive indices, finding application

in optical fibers, optical devices, and lasers.<sup>125</sup> In the past decade, various regular photonic MOF structures were presented.<sup>126,127</sup>

For the photomodulation of the characteristics of one dimensional photonic crystals, also referred to as Bragg stacks, materials with switchable refractive indexes are required. Because of the small surface roughness of SURMOFs, the refractive index of the material can be determined in a straightforward manner by spectroscopic ellipsometry.<sup>42,128</sup> It was found that the refractive index of fluorinated AB SURMOF can be reversibly switched between 1.58 (*trans*) and 1.56 (*cis*) at 600 nm and between 1.73 (*trans*) and 1.65 (*cis*) at 355 nm. On the basis of the well defined structure, DFT calculations were able to unveil the observed phenomena. Because of the large orbital delocalizations and the large transition dipole moment, the *trans*  $\pi-\pi^*$  band has the strongest absorption intensity, stronger than that of any other *cis* absorption band. With the Kramers–Kronig relation, the refractive index and its changes can be calculated, verifying the experimental data.

A five layered TiO<sub>2</sub>/AB SURMOF film was prepared on silicon where each layer has a thickness of approximately 0.5  $\mu\text{m}$  (Figure 9).<sup>71</sup> In the scanning electron microscopy (SEM) images and energy dispersive X ray spectroscopy (EDX) mapping (Figure 9b), a multilayered structure with some periodicity can be seen. Since the refractive indexes of TiO<sub>2</sub> (about 2) and of the fluorinated AB SURMOF differ, the multilayered film may work as a one dimensional photonic crystal or a Bragg reflector. The reflection spectrum shows clear features of a Bragg reflector, although the quality is fairly low, presumably due to deviations of the individual layer thicknesses and the small numbers of layers. Nevertheless, a clear photomodulation of the Bragg reflexes upon *trans*–*cis* photo switching in the SURMOF was observed. The strongest Bragg peak shows a reversible shift by 4 nm to smaller wavelengths upon *trans*–*cis* switching.

## CONCLUSIONS AND OUTLOOK

In the past decade, modular framework materials such as MOFs were explored for their uses as photoswitchable materials. While photoswitchable MOFs in the form of powders are very interesting for switchable adsorption and catalysis,<sup>17</sup> thin films of photoswitchable MOFs have shown to be a valuable model system for the exploration of physicochemical phenomena and advanced experiments. The layer by layer film synthesis, resulting in SURMOF thin films which can be grown on various substrates, is particularly attractive. The high transparency of the SURMOF films enables UV–vis and IR spectroscopic investigations, representing a straightforward tool for the quantification of the photoisomerization. The small film thickness also results in the entire illumination and photo switching of the sample, although the light penetration depth in such MOF materials is typically only in the range of 1  $\mu\text{m}$ . By fabricating membranes where the photoswitchable MOF thin films are grown on mesoporous supports, molecular mixtures can be separated and the selectivity can be remote controlled by light. Moreover, photoswitchable MOF thin films were presented where the electronic and protonic conduction can be modulated with large magnitudes. Photoswitchable SURMOF Bragg stacks were also presented, showing the versatility of potential applications. So far, azobenzene is the functional moiety in most photoswitchable MOF films, and a few studies employing spiropyran were also published. In both cases, changes of the dipole moment rather than changes of the molecular shape seem to dominate the switching effects.

Although we believe in the large potential of photoswitchable MOF films, some drawbacks need to be addressed. On one hand, the research on SURMOF is still in its infancy. The SURMOF synthesis is somewhat more complex than one pot solvothermal MOF synthesis, and only a minority of the known MOF structures have been prepared as SURMOFs so far. While roughly 100 000 MOF structures have been published,<sup>129</sup> the number of SURMOF structures is less than 1000. To date, photoswitchable MOF films possess an even smaller structural diversity (Table 1). So far, most structures are from the pillared layer MOF family, typically with Cu dimer metal nodes. In a few studies, “standard” MOFs such as HKUST 1, ZIF 8, and UiO 67 were used as passive host for the photoswitches. Along with the small diversity comes limited stability. While numerous robust MOFs have been presented,<sup>130</sup> the published photo switchable thin films have limited stability toward long term humidity exposure. We believe that robust, water stable, photoswitchable MOF films, for example, those based on Zr nodes, will be realized soon, allowing membrane separation in aqueous media.

For the future, we believe the field of photoswitchable MOFs will become more diverse. Presumably, more research will focus on membrane separation and on proton and ion conduction as well as on the integration in advanced devices. In addition to the workhorses, AB and SP, more advanced and more specified photoswitches will be used, such as DAE, fulgide, and more. We believe that multiresponsive MOF films will be explored where, in addition to light, other external stimuli such as electric and magnetic fields and heat are employed. Moreover, multifunctional MOF films with several functional moieties in the MOF structure will be explored. The complexity of such multifunctional MOF films will be far beyond that of the presented photoswitchable chiral MOF film. Polarized light may be used to address specific, oriented photoswitches in the MOF film. With

all of these unexplored tasks, we believe that photoswitchable MOF films will remain a very dynamic field and that SURMOFs will make valuable contributions.

## AUTHOR INFORMATION

### Corresponding Author

Lars Heinke – Karlsruhe Institute of Technology (KIT),  
Institute of Functional Interfaces (IFG), 76344 Eggenstein  
Leopoldshafen, Germany; orcid.org/0000 0002 1439  
9695; Email: lars.heinke@kit.edu

### Author

Yunzhe Jiang – Karlsruhe Institute of Technology (KIT),  
Institute of Functional Interfaces (IFG), 76344 Eggenstein  
Leopoldshafen, Germany

### Notes

The authors declare no competing financial interest.

### Biographies

Yunzhe Jiang received his B.Sc. in 2013 from Nanjing University and M.Sc. in chemistry from East China Normal University in 2019. Subsequently, he joined Lars Heinke’s group at Karlsruhe Institute of Technology (KIT) as a Ph.D. student. His current research focuses on developing new structures of photoswitchable SURMOFs.

Lars Heinke studied physics in Greifswald and Leipzig and obtained his Ph.D. from Leipzig University in 2009. After postdoctoral stays at the Fritz Haber Institute in Berlin and at the Lawrence Berkeley National Laboratory, California, he joined the Institute of Functional Interfaces at the KIT as a group leader. His research foci comprise functional nanoporous films and their physicochemical properties, in particular, conduction and diffusion, as well as photoresponsive smart coatings.

## ACKNOWLEDGMENTS

We are grateful to the China Scholarship Council (CSC) and the German Research Foundation (DFG HE 7036/5 and HE7036/6) for financial support.

## REFERENCES

- (1) Stuart, M. A.; Huck, W. T.; Genzer, J.; Müller, M.; Ober, C.; Stamm, M.; Sukhorukov, G. B.; Szleifer, I.; Tsukruk, V. V.; Urban, M.; Winnik, F.; Zauscher, S.; Luzinov, I.; Minko, S. Emerging Applications of Stimuli Responsive Polymer Materials. *Nat. Mater.* **2010**, *9* (2), 101–113.
- (2) Kahn, J. S.; Hu, Y.; Willner, I. Stimuli Responsive DNA Based Hydrogels: From Basic Principles to Applications. *Acc. Chem. Res.* **2017**, *50* (4), 680–690.
- (3) Wang, Y.; Runnerstrom, E. L.; Milliron, D. J. Switchable Materials for Smart Windows. *Annu. Rev. Chem. Biomol. Eng.* **2016**, *7*, 283–304.
- (4) Manrique Juárez, M. D.; Rat, S.; Salmon, L.; Molnár, G.; Quintero, C. M.; Nicu, L.; Shepherd, H. J.; Bousseksou, A. Switchable Molecule Based Materials for Micro and Nanoscale Actuating Applications: Achievements and Prospects. *Coord. Chem. Rev.* **2016**, *308*, 395–408.
- (5) Karmakar, A.; Samanta, P.; Desai, A. V.; Ghosh, S. K. Guest Responsive Metal Organic Frameworks as Scaffolds for Separation and Sensing Applications. *Acc. Chem. Res.* **2017**, *50* (10), 2457–2469.
- (6) Wieme, J.; Lejaeghere, K.; Kresse, G.; Van Speybroeck, V. Tuning the Balance between Dispersion and Entropy to Design Temperature Responsive Flexible Metal Organic Frameworks. *Nat. Commun.* **2018**, *9* (1), 4899.
- (7) Sussardi, A.; Hobday, C. L.; Marshall, R. J.; Forgan, R. S.; Jones, A. C.; Moggach, S. A. Correlating Pressure Induced Emission Modulation with Linker Rotation in a Photoluminescent MOF. *Angew. Chem., Int. Ed.* **2020**, *59* (21), 8118–8122.
- (8) Goulet Hanssens, A.; Eisenreich, F.; Hecht, S. Enlightening Materials with Photoswitches. *Adv. Mater.* **2020**, *32*, 1905966.
- (9) Haldar, R.; Heinke, L.; Wöll, C. Advanced Photoresponsive Materials Using the Metal Organic Framework Approach. *Adv. Mater.* **2020**, *32*, 1905227.
- (10) Feringa, B. L.; van Delden, R. A.; Koumura, N.; Geertsema, E. M. Chiroptical Molecular Switches. *Chem. Rev.* **2000**, *100* (5), 1789–1816.
- (11) Feringa, B. L. The Art of Building Small: From Molecular Switches to Molecular Motors. *J. Org. Chem.* **2007**, *72* (18), 6635–6652.
- (12) Pianowski, Z. L. Recent Implementations of Molecular Photoswitches into Smart Materials and Biological Systems. *Chem. Eur. J.* **2019**, *25* (20), S128–S144.
- (13) Gu, Y.; Alt, E. A.; Wang, H.; Li, X.; Willard, A. P.; Johnson, J. A. Photoswitching Topology in Polymer Networks with Metal Organic Cages as Crosslinks. *Nature* **2018**, *560* (7716), 65–69.
- (14) Asshoff, S. J.; Lancia, F.; Iamsaard, S.; Matt, B.; Kudernac, T.; Fletcher, S. P.; Katsonis, N. High Power Actuation from Molecular Photoswitches in Enantiomerically Paired Soft Springs. *Angew. Chem., Int. Ed.* **2017**, *56* (12), 3261–3265.
- (15) Rice, A. M.; Martin, C. R.; Galitskiy, V. A.; Berseneva, A. A.; Leith, G. A.; Shustova, N. B. Photophysics Modulation in Photo switchable Metal Organic Frameworks. *Chem. Rev.* **2020**, *120* (16), 8790–8813.
- (16) Das, G.; Prakasam, T.; Addicoat, M. A.; Sharma, S. K.; Ravoux, F.; Mathew, R.; Baias, M.; Jagannathan, R.; Olson, M. A.; Trabolsi, A. Azobenzene Equipped Covalent Organic Framework: Light Operated Reservoir. *J. Am. Chem. Soc.* **2019**, *141* (48), 19078–19087.
- (17) Bigdeli, F.; Lollar, C. T.; Morsali, A.; Zhou, H. C. Switching in Metal Organic Frameworks. *Angew. Chem., Int. Ed.* **2020**, *59* (12), 4652–4669.
- (18) Zhou, H. C.; Kitagawa, S. Metal Organic Frameworks (MOFs). *Chem. Soc. Rev.* **2014**, *43* (16), 5415–5418.
- (19) Furukawa, H.; Cordova, K. E.; O’Keeffe, M.; Yaghi, O. M. The Chemistry and Applications of Metal Organic Frameworks. *Science* **2013**, *341* (6149), 1230444.
- (20) Furukawa, H.; Ko, N.; Go, Y. B.; Aratani, N.; Choi, S. B.; Choi, E.; Yazaydin, A. Ö.; Snurr, R. Q.; O’Keeffe, M.; Kim, J.; Yaghi, O. M. Ultrahigh Porosity in Metal Organic Frameworks. *Science* **2010**, *329* (5990), 424.
- (21) Jia, J.; Sun, F.; Fang, Q.; Liang, X.; Cai, K.; Bian, Z.; Zhao, H.; Gao, L.; Zhu, G. A Novel Low Density Metal Organic Framework with PCU Topology by Dendritic Ligand. *Chem. Commun.* **2011**, *47* (32), 9167–9169.
- (22) Lian, X.; Fang, Y.; Joseph, E.; Wang, Q.; Li, J.; Banerjee, S.; Lollar, C.; Wang, X.; Zhou, H. C. Enzyme MOF (Metal Organic Framework) Composites. *Chem. Soc. Rev.* **2017**, *46* (11), 3386–3401.
- (23) Cavka, J. H.; Jakobsen, S.; Olsbye, U.; Guillou, N.; Lamberti, C.; Bordiga, S.; Lillerud, K. P. A New Zirconium Inorganic Building Brick Forming Metal Organic Frameworks with Exceptional Stability. *J. Am. Chem. Soc.* **2008**, *130* (42), 13850–13851.
- (24) Denny, M. S., Jr; Moreton, J. C.; Benz, L.; Cohen, S. M. Metal Organic Frameworks for Membrane Based Separations. *Nat. Rev. Mater.* **2016**, *1*, 16078.
- (25) Qiu, S.; Xue, M.; Zhu, G. Metal Organic Framework Membranes: From Synthesis to Separation Application. *Chem. Soc. Rev.* **2014**, *43* (16), 6116–6140.
- (26) Bux, H.; Chmelik, C.; Krishna, R.; Caro, J. Ethene/Ethane Separation by the MOF Membrane ZIF 8: Molecular Correlation of Permeation, Adsorption, Diffusion. *J. Membr. Sci.* **2011**, *369* (1–2), 284–289.
- (27) Falcaro, P.; Ricco, R.; Doherty, C. M.; Liang, K.; Hill, A. J.; Styles, M. J. MOF Positioning Technology and Device Fabrication. *Chem. Soc. Rev.* **2014**, *43* (16), 5513–5560.
- (28) Stassen, I.; Styles, M.; Greci, G.; Gorp, H. V.; Vanderlinden, W.; Feyter, S. D.; Falcaro, P.; Vos, D. D.; Vereecken, P.; Ameloot, R. Chemical Vapour Deposition of Zeolitic Imidazolate Framework Thin Films. *Nat. Mater.* **2016**, *15* (3), 304–310.
- (29) Falcaro, P.; Okada, K.; Hara, T.; Ikigaki, K.; Tokudome, Y.; Thornton, A. W.; Hill, A. J.; Williams, T.; Doonan, C.; Takahashi, M. Centimetre Scale Micropore Alignment in Oriented Polycrystalline Metal Organic Framework Films via Heteroepitaxial Growth. *Nat. Mater.* **2017**, *16* (3), 342–348.
- (30) Shekhah, O.; Wang, H.; Kowarik, S.; Schreiber, F.; Paulus, M.; Tolan, M.; Sternemann, C.; Evers, F.; Zacher, D.; Fischer, R. A.; Wöll, C. Step by Step Route for the Synthesis of Metal Organic Frameworks. *J. Am. Chem. Soc.* **2007**, *129* (49), 15118–15119.
- (31) Shekhah, O. Layer by Layer Method for the Synthesis and Growth of Surface Mounted Metal Organic Frameworks (SURMOFs). *Materials* **2010**, *3* (2), 1302–1315.
- (32) Shekhah, O.; Liu, J.; Fischer, R. A.; Wöll, C. MOF Thin Films: Existing and Future Applications. *Chem. Soc. Rev.* **2011**, *40* (2), 1081–1106.
- (33) Zacher, D.; Schmid, R.; Wöll, C.; Fischer, R. A. Surface Chemistry of Metal Organic Frameworks at the Liquid Solid Interface. *Angew. Chem., Int. Ed.* **2011**, *50* (1), 176–199.
- (34) Stavila, V.; Volponi, J.; Katzenmeyer, A. M.; Dixon, M. C.; Allendorf, M. D. Kinetics and Mechanism of Metal Organic Framework Thin Film Growth: Systematic Investigation of HKUST 1 Deposition on QCM Electrodes. *Chem. Sci.* **2012**, *3* (5), 1531.
- (35) John, N. S.; Scherb, C.; Shöäë, M.; Anderson, M. W.; Attfield, M. P.; Bein, T. Single Layer Growth of Sub Micron Metal Organic Framework Crystals Observed by in situ Atomic Force Microscopy. *Chem. Commun.* **2009**, *41*, 6294–6296.
- (36) Rivera Torrente, M.; Mandemaker, L. D. B.; Filez, M.; Delen, G.; Seoane, B.; Meirer, F.; Weckhuysen, B. M. Spectroscopy, Microscopy, Diffraction and Scattering of Archetypal MOFs: Formation, Metal Sites in Catalysis and Thin Films. *Chem. Soc. Rev.* **2020**, *49* (18), 6694–6732.
- (37) Shekhah, O.; Wang, H.; Zacher, D.; Fischer, R. A.; Wöll, C. Growth Mechanism of Metal Organic Frameworks: Insights into the Nucleation by Employing a Step by Step Route. *Angew. Chem., Int. Ed.* **2009**, *48* (27), 5038–5041.
- (38) Heinke, L.; Gu, Z.; Wöll, C. The Surface Barrier Phenomenon at the Loading of Metal Organic Frameworks. *Nat. Commun.* **2014**, *5*, 4562.

- (39) Zhuang, J. L.; Kind, M.; Grytz, C. M.; Farr, F.; Diefenbach, M.; Tussupbayev, S.; Holthausen, M. C.; Terfort, A. Insight into the Oriented Growth of Surface Attached Metal Organic Frameworks: Surface Functionality, Deposition Temperature, and First Layer Order. *J. Am. Chem. Soc.* **2015**, *137* (25), 8237–8243.
- (40) Zhuang, J. L.; Terfort, A.; Wöll, C. Formation of Oriented and Patterned Films of Metal Organic Frameworks by Liquid Phase Epitaxy: A Review. *Coord. Chem. Rev.* **2016**, *307*, 391–424.
- (41) St. Petkov, P.; Vayssilov, G. N.; Liu, J.; Shekhah, O.; Wang, Y.; Woll, C.; Heine, T. Defects in MOFs: A Thorough Characterization. *ChemPhysChem* **2012**, *13* (8), 2025–2029.
- (42) Gu, Z. G.; Pfriem, A.; Hamsch, S.; Breitwieser, H.; Wohlgenuth, J.; Heinke, L.; Gliemann, H.; Wöll, C. Transparent Films of Metal Organic Frameworks for Optical Applications. *Microporous Mesoporous Mater.* **2015**, *211*, 82–87.
- (43) Müller, K.; Fink, K.; Schottner, L.; Koenig, M.; Heinke, L.; Wöll, C. Defects as Color Centers: The Apparent Color of Metal Organic Frameworks Containing Cu<sup>2+</sup> Based Paddle Wheel Units. *ACS Appl. Mater. Interfaces* **2017**, *9* (42), 37463–37467.
- (44) Heinke, L.; Wöll, C. Surface Mounted Metal Organic Frameworks: Crystalline and Porous Molecular Assemblies for Fundamental Insights and Advanced Applications. *Adv. Mater.* **2019**, *31* (26), 1806324.
- (45) Mandemaker, L. D. B.; Rivera Torrente, M.; Geitner, R.; Vis, C. M.; Weckhuysen, B. M. In situ Spectroscopy of Calcium Fluoride Anchored Metal Organic Framework Thin Films During Gas Sorption. *Angew. Chem., Int. Ed.* **2020**, *59*, 19545–19552.
- (46) Cakici, M.; Gu, Z. G.; Nieger, M.; Burck, J.; Heinke, L.; Bräse, S. Planar Chiral Building Blocks for Metal Organic Frameworks. *Chem. Commun. (Cambridge, U. K.)* **2015**, *51* (23), 4796–4798.
- (47) Tu, M.; Wannapaiboon, S.; Fischer, R. A. Programmed Functionalization of SURMOFs via Liquid Phase Heteroepitaxial Growth and Post Synthetic Modification. *Dalton Trans.* **2013**, *42* (45), 16029–35.
- (48) Delen, G.; Ristanović, Z.; Mandemaker, L. D. B.; Weckhuysen, B. M. Mechanistic Insights into Growth of Surface Mounted Metal Organic Framework Films Resolved by Infrared (Nano ) Spectroscopy. *Chem. Eur. J.* **2018**, *24* (1), 187–195.
- (49) Heinke, L.; Cakici, M.; Dommaschk, M.; Grosjean, S.; Herges, R.; Bräse, S.; Wöll, C. Photoswitching in Two Component Surface Mounted Metal Organic Frameworks: Optically Triggered Release from a Molecular Container. *ACS Nano* **2014**, *8* (2), 1463–1467.
- (50) Sun, L.; Campbell, M. G.; Dinca, M. Electrically Conductive Porous Metal Organic Frameworks. *Angew. Chem., Int. Ed.* **2016**, *55* (11), 3566–79.
- (51) Sun, L.; Park, S. S.; Sheberla, D.; Dinca, M. Measuring and Reporting Electrical Conductivity in Metal Organic Frameworks: Cd<sub>2</sub>(TTFB) as a Case Study. *J. Am. Chem. Soc.* **2016**, *138* (44), 14772–14782.
- (52) Stavila, V.; Talin, A. A.; Allendorf, M. D. MOF Based Electronic and Opto Electronic Devices. *Chem. Soc. Rev.* **2014**, *43* (16), 5994–6010.
- (53) Dolgoplova, E. A.; Galitskiy, V. A.; Martin, C. R.; Gregory, H. N.; Yarbrough, B. J.; Rice, A. M.; Berseneva, A. A.; Elegbawo, O. A.; Stephenson, K. S.; Kittikhunnatham, P.; Karakalos, S. G.; Smith, M. D.; Greytak, A. B.; Garashchuk, S.; Shustova, N. B. Connecting Wires: Photoinduced Electronic Structure Modulation in Metal Organic Frameworks. *J. Am. Chem. Soc.* **2019**, *141* (13), 5350–5358.
- (54) Fan, C. B.; Liu, Z. Q.; Gong, L. L.; Zheng, A. M.; Zhang, L.; Yan, C. S.; Wu, H. Q.; Feng, X. F.; Luo, F. Photoswitching Adsorption Selectivity in a Diarylethene Azobenzene MOF. *Chem. Commun. (Cambridge, U. K.)* **2017**, *53* (4), 763–766.
- (55) Luo, F.; Fan, C. B.; Luo, M. B.; Wu, X. L.; Zhu, Y.; Pu, S. Z.; Xu, W. Y.; Guo, G. C. Photoswitching CO<sub>2</sub> Capture and Release in a Photochromic Diarylethene Metal Organic Framework. *Angew. Chem., Int. Ed.* **2014**, *53* (35), 9298–301.
- (56) Wang, Z.; Grosjean, S.; Bräse, S.; Heinke, L. Photoswitchable Adsorption in Metal Organic Frameworks Based on Polar Guest Host Interactions. *ChemPhysChem* **2015**, *16* (18), 3779–83.
- (57) Kanj, A. B.; Bürck, J.; Grosjean, S.; Bräse, S.; Heinke, L. Switching the Enantioselectivity of Nanoporous Host Materials by Light. *Chem. Commun.* **2019**, *55* (60), 8776–8779.
- (58) Müller, K.; Wadhwa, J.; Singh Malhi, J.; Schottner, L.; Welle, A.; Schwartz, H.; Hermann, D.; Ruschewitz, U.; Heinke, L. Photo switchable Nanoporous Films by Loading Azobenzene in Metal Organic Frameworks of Type HKUST 1. *Chem. Commun.* **2017**, *53* (57), 8070–8073.
- (59) Wang, Z. B.; Müller, K.; Valasek, M.; Grosjean, S.; Bräse, S.; Wöll, C.; Mayor, M.; Heinke, L. Series of Photoswitchable Azobenzene Containing Metal Organic Frameworks with Variable Adsorption Switching Effect. *J. Phys. Chem. C* **2018**, *122* (33), 19044–19050.
- (60) Wang, Z.; Knebel, A.; Grosjean, S.; Wagner, D.; Bräse, S.; Wöll, C.; Caro, J.; Heinke, L. Tunable Molecular Separation by Nanoporous Membranes. *Nat. Commun.* **2016**, *7*, 13872.
- (61) Knebel, A.; Sundermann, L.; Mohmeyer, A.; Strauss, I.; Friebe, S.; Behrens, P.; Caro, J. Azobenzene Guest Molecules as Light Switchable CO<sub>2</sub> Valves in an Ultrathin UiO 67 Membrane. *Chem. Mater.* **2017**, *29* (7), 3111–3117.
- (62) Müller, K.; Knebel, A.; Zhao, F. L.; Bleger, D.; Caro, J.; Heinke, L. Switching Thin Films of Azobenzene Containing Metal Organic Frameworks with Visible Light. *Chem. Eur. J.* **2017**, *23* (23), 5434–5438.
- (63) Müller, K.; Helfferich, J.; Zhao, F. L.; Verma, R.; Kanj, A. B.; Meded, V.; Bleger, D.; Wenzel, W.; Heinke, L. Switching the Proton Conduction in Nanoporous, Crystalline Materials by Light. *Adv. Mater.* **2018**, *30* (8), 1706551.
- (64) Kanj, A. B.; Chandresh, A.; Gerwien, A.; Grosjean, S.; Bräse, S.; Wang, Y.; Dube, H.; Heinke, L. Proton Conduction Photomodulation in Spiropyran Functionalized MOFs with Large on off Ratio. *Chem. Sci.* **2020**, *11* (5), 1404–1410.
- (65) Liang, H. Q.; Guo, Y.; Shi, Y.; Peng, X.; Liang, B.; Chen, B. A Light Responsive Metal Organic Framework Hybrid Membrane with High on/off Photoswitchable Proton Conductivity. *Angew. Chem., Int. Ed.* **2020**, *59* (20), 7732–7737.
- (66) Liang, H. Q.; Guo, Y.; Peng, X.; Chen, B. Light Gated Cation Selective Transport in Metal Organic Framework Membranes. *J. Mater. Chem. A* **2020**, *8* (22), 11399–11405.
- (67) Garg, S.; Schwartz, H.; Kozłowska, M.; Kanj, A. B.; Müller, K.; Wenzel, W.; Ruschewitz, U.; Heinke, L. Conductance Photoswitching of Metal Organic Frameworks with Embedded Spiropyran. *Angew. Chem., Int. Ed.* **2019**, *58* (4), 1193–1197.
- (68) Yu, X. J.; Wang, Z. B.; Buchholz, M.; Füllgrabe, N.; Grosjean, S.; Bebensee, F.; Bräse, S.; Wöll, C.; Heinke, L. Cis to trans Isomerization of Azobenzene Investigated by Using Thin Films of Metal Organic Frameworks. *Phys. Chem. Chem. Phys.* **2015**, *17* (35), 22721–22725.
- (69) Wang, Z.; Heinke, L.; Jelic, J.; Cakici, M.; Dommaschk, M.; Maurer, R. J.; Oberhofer, H.; Grosjean, S.; Herges, R.; Bräse, S.; Reuter, K.; Wöll, C. Photoswitching in Nanoporous, Crystalline Solids: An Experimental and Theoretical Study for Azobenzene Linkers Incorporated in MOFs. *Phys. Chem. Chem. Phys.* **2015**, *17* (22), 14582–14587.
- (70) Zhang, F.; Zou, X.; Feng, W.; Zhao, X.; Jing, X.; Sun, F.; Ren, H.; Zhu, G. Microwave Assisted Crystallization Inclusion of Spiropyran Molecules in Indium Trimesate Films with Antidromic Reversible Photochromism. *J. Mater. Chem.* **2012**, *22* (48), 25019.
- (71) Zhang, Z. J.; Müller, K.; Heidrich, S.; Koenig, M.; Hashem, T.; Schloder, T.; Bleger, D.; Wenzel, W.; Heinke, L. Light Switchable One Dimensional Photonic Crystals Based on MOFs with Photomodulatable Refractive Index. *J. Phys. Chem. Lett.* **2019**, *10* (21), 6626–6633.
- (72) Liu, X.; Kozłowska, M.; Okkali, T.; Wagner, D.; Higashino, T.; Brenner Weiß, G.; Marschner, S. M.; Fu, Z.; Zhang, Q.; Imahori, H.; Bräse, S.; Wenzel, W.; Wöll, C.; Heinke, L. Photoconductivity in Metal Organic Framework (MOF) Thin Films. *Angew. Chem., Int. Ed.* **2019**, *58* (28), 9590–9595.
- (73) Schwartz, H. A.; Werker, M.; Tobeck, C.; Christoffels, R.; Schaniel, D.; Olthof, S.; Meerholz, K.; Kopacka, H.; Huppertz, H.; Ruschewitz, U. Novel Photoactive Spirooxazine Based Switch@MOF Composite Materials. *ChemPhotoChem.* **2020**, *4* (3), 195–206.

- (74) Schwartz, H. A.; Olthof, S.; Schaniel, D.; Meerholz, K.; Ruschewitz, U. Solution Like Behavior of Photoswitchable Spiropyran Embedded in Metal Organic Frameworks. *Inorg. Chem.* **2017**, *56* (21), 13100–13110.
- (75) Schwartz, H. A.; Ruschewitz, U.; Heinke, L. Smart Nanoporous Metal Organic Frameworks by Embedding Photochromic Molecules State of the Art and Future Perspectives. *Photochem. Photobiol. Sci.* **2018**, *17* (7), 864–873.
- (76) Schaate, A.; Dühnen, S.; Platz, G.; Lilienthal, S.; Schneider, A. M.; Behrens, P. A Novel Zr Based Porous Coordination Polymer Containing Azobenzenedicarboxylate as a Linker. *Eur. J. Inorg. Chem.* **2012**, *2012* (5), 790–796.
- (77) Kanj, A. B.; Müller, K.; Heinke, L. Stimuli Responsive Metal Organic Frameworks with Photoswitchable Azobenzene Side Groups. *Macromol. Rapid Commun.* **2018**, *39* (1), 1700239.
- (78) Bleger, D.; Schwarz, J.; Brouwer, A. M.; Hecht, S. O Fluoroazobenzenes as Readily Synthesized Photoswitches Offering Nearly Quantitative Two Way Isomerization with Visible Light. *J. Am. Chem. Soc.* **2012**, *134* (51), 20597–600.
- (79) Wang, Z.; Cohen, S. M. Postsynthetic Modification of Metal Organic Frameworks. *Chem. Soc. Rev.* **2009**, *38* (5), 1315–29.
- (80) Kolb, H. C.; Finn, M. G.; Sharpless, K. B. Click Chemistry: Diverse Chemical Function from a Few Good Reactions. *Angew. Chem., Int. Ed.* **2001**, *40* (11), 2004–2021.
- (81) Kumar, G. S.; Neckers, D. Photochemistry of Azobenzene Containing Polymers. *Chem. Rev.* **1989**, *89* (8), 1915–1925.
- (82) Klajn, R. Spiropyran Based Dynamic Materials. *Chem. Soc. Rev.* **2014**, *43* (1), 148–84.
- (83) Crespi, S.; Simeth, N. A.; König, B. Heteroaryl Azo Dyes as Molecular Photoswitches. *Nat. Rev. Chem.* **2019**, *3* (3), 133–146.
- (84) Huang, H.; Sato, H.; Aida, T. Crystalline Nanochannels with Pendant Azobenzene Groups: Steric or Polar Effects on Gas Adsorption and Diffusion? *J. Am. Chem. Soc.* **2017**, *139* (26), 8784–8787.
- (85) Mutruc, D.; Goulet Hanssens, A.; Fairman, S.; Wahl, S.; Zimathies, A.; Knie, C.; Hecht, S. Modulating Guest Uptake in Core Shell MOFs with Visible Light. *Angew. Chem., Int. Ed.* **2019**, *58* (37), 12862–12867.
- (86) Zhou, W.; Grosjean, S.; Bräse, S.; Heinke, L. Thermal cis to trans Isomerization of Azobenzene Side Groups in Metal Organic Frameworks Investigated by Localized Surface Plasmon Resonance Spectroscopy. *Z. Phys. Chem. (Muenchen, Ger.)* **2018**, *233* (1), 15–22.
- (87) Li, H.; Wang, K.; Sun, Y.; Lollar, C. T.; Li, J.; Zhou, H. C. Recent Advances in Gas Storage and Separation Using Metal Organic Frameworks. *Mater. Today* **2018**, *21* (2), 108–121.
- (88) Mukherjee, S.; Sensharma, D.; Chen, K. J.; Zaworotko, M. J. Crystal Engineering of Porous Coordination Networks to Enable Separation of C<sub>2</sub> Hydrocarbons. *Chem. Commun.* **2020**, *56* (72), 10419–10441.
- (89) Park, J.; Yuan, D. Q.; Pham, K. T.; Li, J. R.; Yakovenko, A.; Zhou, H. C. Reversible Alteration of CO<sub>2</sub> Adsorption Upon Photochemical or Thermal Treatment in a Metal Organic Framework. *J. Am. Chem. Soc.* **2012**, *134* (1), 99–102.
- (90) Nandasiri, M. I.; Jambovane, S. R.; McGrail, B. P.; Schaefer, H. T.; Nune, S. K. Adsorption, Separation, and Catalytic Properties of Densified Metal Organic Frameworks. *Coord. Chem. Rev.* **2016**, *311*, 38–52.
- (91) Valadez Sanchez, E. P.; Knebel, A.; Izquierdo Sanchez, L.; Klumpp, M.; Wöll, C.; Dittmeyer, R. Studying ZIF 8 SURMOF Thin Films with a Langatate Crystal Microbalance: Single Component Gas Adsorption Isotherms Measured at Elevated Temperatures and Pressures. *Langmuir* **2020**, *36* (29), 8444–8450.
- (92) Müller, K.; Vankova, N.; Schottner, L.; Heine, T.; Heinke, L. Dissolving Uptake Hindering Surface Defects in Metal Organic Frameworks. *Chem. Sci.* **2019**, *10* (1), 153–160.
- (93) Johannsmann, D. The Quartz Crystal Microbalance in Soft Matter Research. *Soft and Biological Matter*; Springer International Publishing: 2015.
- (94) Zybalyo, O.; Shekhah, O.; Wang, H.; Tafipolsky, M.; Schmid, R.; Johannsmann, D.; Wöll, C. A Novel Method to Measure Diffusion Coefficients in Porous Metal Organic Frameworks. *Phys. Chem. Chem. Phys.* **2010**, *12* (28), 8092–7.
- (95) Li, C.; Heinke, L. Thin Films of Homochiral Metal Organic Frameworks for Chiroptical Spectroscopy and Enantiomer Separation. *Symmetry* **2020**, *12* (5), 686.
- (96) Sorribas, S.; Gorgojo, P.; Tellez, C.; Coronas, J.; Livingston, A. G. High Flux Thin Film Nanocomposite Membranes Based on Metal Organic Frameworks for Organic Solvent Nanofiltration. *J. Am. Chem. Soc.* **2013**, *135* (40), 15201–8.
- (97) Shah, M.; McCarthy, M. C.; Sachdeva, S.; Lee, A. K.; Jeong, H. K. Current Status of Metal Organic Framework Membranes for Gas Separations: Promises and Challenges. *Ind. Eng. Chem. Res.* **2012**, *51* (5), 2179–2199.
- (98) Li, X.; Liu, Y.; Wang, J.; Gascon, J.; Li, J.; Van der Bruggen, B. Metal Organic Frameworks Based Membranes for Liquid Separation. *Chem. Soc. Rev.* **2017**, *46* (23), 7124–7144.
- (99) Aceituno Melgar, V. M.; Kim, J.; Othman, M. R. Zeolitic Imidazolate Framework Membranes for Gas Separation: A Review of Synthesis Methods and Gas Separation Performance. *J. Ind. Eng. Chem.* **2015**, *28*, 1–15.
- (100) Caro, J. Quo Vadis, MOF? *Chem. Ing. Tech.* **2018**, *90* (11), 1759–1768.
- (101) Rangnekar, N.; Mittal, N.; Elyassi, B.; Caro, J.; Tsapatsis, M. Zeolite Membranes a Review and Comparison with MOFs. *Chem. Soc. Rev.* **2015**, *44* (20), 7128–54.
- (102) Hurrle, S.; Friebe, S.; Wohlgemuth, J.; Wöll, C.; Caro, J.; Heinke, L. Sprayable, Large Area Metal Organic Framework Films and Membranes of Varying Thickness. *Chem. Eur. J.* **2017**, *23* (10), 2294–2298.
- (103) Liu, C.; Jiang, Y.; Zhou, C.; Caro, J.; Huang, A. Photo Switchable Smart Metal Organic Framework Membranes with Tunable and Enhanced Molecular Sieving Performance. *J. Mater. Chem. A* **2018**, *6* (48), 24949–24955.
- (104) Vankelecom, I. F. J.; Merckx, E.; Luts, M.; Uytterhoeven, J. B. Incorporation of Zeolites in Polyimide Membranes. *J. Phys. Chem.* **1995**, *99* (35), 13187–13192.
- (105) Zimmerman, C. M.; Singh, A.; Koros, W. J. Tailoring Mixed Matrix Composite Membranes for Gas Separations. *J. Membr. Sci.* **1997**, *137* (1), 145–154.
- (106) Dechnik, J.; Gascon, J.; Doonan, C. J.; Janiak, C.; Sumby, C. J. Mixed Matrix Membranes. *Angew. Chem., Int. Ed.* **2017**, *56* (32), 9292–9310.
- (107) Prasetya, N.; Ladewig, B. P. An Insight into the Effect of Azobenzene Functionalities Studied in UiO 66 Frameworks for Low Energy CO<sub>2</sub> Capture and CO<sub>2</sub>/N<sub>2</sub> Membrane Separation. *J. Mater. Chem. A* **2019**, *7* (25), 15164–15172.
- (108) Prasetya, N.; Ladewig, B. P. New Azo DMOF 1 MOF as a Photoresponsive Low Energy CO<sub>2</sub> Adsorbent and Its Exceptional CO<sub>2</sub>/N<sub>2</sub> Separation Performance in Mixed Matrix Membranes. *ACS Appl. Mater. Interfaces* **2018**, *10* (40), 34291–34301.
- (109) Prasetya, N.; Teck, A. A.; Ladewig, B. P. Matrimid JUC 62 and Matrimid PCN 250 Mixed Matrix Membranes Displaying Light Responsive Gas Separation and Beneficial Ageing Characteristics for CO<sub>2</sub>/N<sub>2</sub> Separation. *Sci. Rep.* **2018**, *8* (1), 2944.
- (110) Stassen, I.; Burtch, N. C.; Talin, A. A.; Falcaro, P.; Allendorf, M. D.; Ameloot, R. An Updated Roadmap for the Integration of Metal Organic Frameworks with Electronic Devices and Chemical Sensors. *Chem. Soc. Rev.* **2017**, *46* (11), 3185–3241.
- (111) Meng, X.; Wang, H. N.; Song, S. Y.; Zhang, H. J. Proton Conducting Crystalline Porous Materials. *Chem. Soc. Rev.* **2017**, *46* (2), 464–480.
- (112) Ramaswamy, P.; Wong, N. E.; Shimizu, G. K. MOFs as Proton Conductors Challenges and Opportunities. *Chem. Soc. Rev.* **2014**, *43* (16), 5913–32.
- (113) Wang, S.; Wahiduzzaman, M.; Davis, L.; Tissot, A.; Shepard, W.; Marrot, J.; Martineau Corcos, C.; Hamdane, D.; Maurin, G.; Devautour Vinot, S.; Serre, C. A Robust Zirconium Amino Acid Metal Organic Framework for Proton Conduction. *Nat. Commun.* **2018**, *9* (1), 4937.

- (114) Patel, H. A.; Mansor, N.; Gadipelli, S.; Brett, D. J.; Guo, Z. Superacidity in Nafion/MOF Hybrid Membranes Retains Water at Low Humidity to Enhance Proton Conduction for Fuel Cells. *ACS Appl. Mater. Interfaces* **2016**, *8* (45), 30687–30691.
- (115) Mendrecki, L.; Mirica, K. A. Conductive Metal Organic Frameworks as Ion to Electron Transducers in Potentiometric Sensors. *ACS Appl. Mater. Interfaces* **2018**, *10* (22), 19248–19257.
- (116) Ramaswamy, P.; Wong, N. E.; Gelfand, B. S.; Shimizu, G. K. A Water Stable Magnesium MOF that Conducts Protons over  $10^{-2}$  S·cm<sup>-1</sup>. *J. Am. Chem. Soc.* **2015**, *137* (24), 7640–3.
- (117) Kim, S.; Dawson, K. W.; Gelfand, B. S.; Taylor, J. M.; Shimizu, G. K. Enhancing Proton Conduction in a Metal Organic Framework by Isomorphous Ligand Replacement. *J. Am. Chem. Soc.* **2013**, *135* (3), 963–6.
- (118) Sun, L.; Miyakai, T.; Seki, S.; Dinca, M. Mn<sub>2</sub>(2,5 Disulphydrylbenzene 1,4 Dicarboxylate): A Microporous Metal Organic Framework with Infinite (Mn S)<sub>∞</sub> Chains and High Intrinsic Charge Mobility. *J. Am. Chem. Soc.* **2013**, *135* (22), 8185–8.
- (119) Leong, C. F.; Chan, B.; Faust, T. B.; D'Alessandro, D. M. Controlling Charge Separation in a Novel Donor Acceptor Metal Organic Framework Via Redox Modulation. *Chem. Sci.* **2014**, *5* (12), 4724–4728.
- (120) Sheberla, D.; Sun, L.; Blood Forsythe, M. A.; Er, S.; Wade, C. R.; Brozek, C. K.; Aspuru Guzik, A.; Dinca, M. High Electrical Conductivity in Ni<sub>3</sub>(2,3,6,7,10,11 hexaminotriphenylene)<sub>2</sub>, a Semi conducting Metal Organic Graphene Analogue. *J. Am. Chem. Soc.* **2014**, *136* (25), 8859–62.
- (121) Talin, A. A.; Centrone, A.; Ford, A. C.; Foster, M. E.; Stavila, V.; Haney, P.; Kinney, R. A.; Szalai, V.; El Gabaly, F.; Yoon, H. P.; Léonard, F.; Allendorf, M. D. Tunable Electrical Conductivity in Metal Organic Framework Thin Film Devices. *Science* **2014**, *343* (6166), 66–69.
- (122) Darwish, N.; Aragones, A. C.; Darwish, T.; Ciampi, S.; Diez Perez, I. Multi Responsive Photo and Chemo Electrical Single Molecule Switches. *Nano Lett.* **2014**, *14* (12), 7064–7070.
- (123) Hou, L.; Leydecker, T.; Zhang, X.; Rekab, W.; Herder, M.; Cendra, C.; Hecht, S.; McCulloch, I.; Salleo, A.; Orgiu, E.; Samori, P. Engineering Optically Switchable Transistors with Improved Performance by Controlling Interactions of Diarylethenes in Polymer Matrices. *J. Am. Chem. Soc.* **2020**, *142* (25), 11050–11059.
- (124) Irie, M.; Fulcaminato, T.; Matsuda, K.; Kobatake, S. Photochromism of Diarylethene Molecules and Crystals: Memories, Switches, and Actuators. *Chem. Rev.* **2014**, *114* (24), 12174–12277.
- (125) López, C. Materials Aspects of Photonic Crystals. *Adv. Mater.* **2003**, *15* (20), 1679–1704.
- (126) Cui, Y.; Zhang, J.; He, H.; Qian, G. Photonic Functional Metal Organic Frameworks. *Chem. Soc. Rev.* **2018**, *47* (15), 5740–5785.
- (127) Avci, C.; Imaz, I.; Carne Sanchez, A.; Pariente, J. A.; Tasios, N.; Perez Carvajal, J.; Alonso, M. I.; Blanco, A.; Dijkstra, M.; Lopez, C.; MasPOCH, D. Self Assembly of Polyhedral Metal Organic Framework Particles into Three Dimensional Ordered Superstructures. *Nat. Chem.* **2018**, *10* (1), 78–84.
- (128) Redel, E.; Wang, Z.; Walheim, S.; Liu, J.; Gliemann, H.; Wöll, C. On the Dielectric and Optical Properties of Surface Anchored Metal Organic Frameworks: A Study on Epitaxially Grown Thin Films. *Appl. Phys. Lett.* **2013**, *103* (9), 091903.
- (129) Moghadam, P. Z.; Li, A.; Liu, X. W.; Bueno Perez, R.; Wang, S. D.; Wiggin, S. B.; Wood, P. A.; Fairen Jimenez, D. Targeted Classification of Metal Organic Frameworks in the Cambridge Structural Database (CSD). *Chem. Sci.* **2020**, *11* (32), 8373–8387.
- (130) Kirchon, A.; Feng, L.; Drake, H. F.; Joseph, E. A.; Zhou, H. C. From Fundamentals to Applications: A Toolbox for Robust and Multifunctional MOF Materials. *Chem. Soc. Rev.* **2018**, *47* (23), 8611–8638.

## Repository KITopen

Dies ist ein Postprint/begutachtetes Manuskript.

Empfohlene Zitierung:

Jiang, Y.; Heinke, L.

[Photoswitchable metal-organic framework thin films: From spectroscopy to remote-controllable membrane separation and switchable conduction.](#)

2021. Langmuir, 37.

doi:[10.5445/IR/1000129353](#)

Zitierung der Originalveröffentlichung:

Jiang, Y.; Heinke, L.

[Photoswitchable metal-organic framework thin films: From spectroscopy to remote-controllable membrane separation and switchable conduction.](#)

2021. Langmuir, 37 (1), 2–15.

doi:[10.1021/acs.langmuir.0c02859](#)

Lizenzinformationen: [KITopen-Lizenz](#)